Modeling of Active Infrared Thermography for Defect Detection in Concrete Structures

B. Cannas[1], S. Carcangiu[*1], G. Concu[2], and N. Trulli[3]
[1] Department of Electric and Electronic Engineering, University of Cagliari,
[2] Department of Civil Engineering, Environmental and Architecture, University of Cagliari
[3] Department of Architecture and Planning, University of Sassari
*Corresponding author: Piazza d'Armi, 09123 Cagliari, Italy, s.carcangiu@diee.unica.it

Abstract: An experimental program has been developed, with the purpose of evaluating the reliability in building diagnosis and characterization of an integrated analysis of several parameters related to heat transfer process through the building material. The Infrared Thermography Technique (IRT) has been applied. Experimental measurements have been carried out on a concrete structure with an inside cavity. Moreover further defects have been inserted in the near surface of the structure at different depth. In this paper the finite element method has been used to simulate by a 3D model the heat transfer process induced into the concrete structure by two halogen lamps in order to detect the position of the defects.

Keywords: Infrared Thermography, Non-Destructive Testing, Finite Element Method, Heat transfer process.

1. Introduction

Inspection and monitoring of structural conditions is an essential part of life-cycle management of civil engineering systems. In the last decades, extend the useful service life of structures and infrastructures has become of crucial importance, due to cultural, social, and economic factors. In the field of assessment methodologies particular importance is given to development of Non-Destructive Testing Techniques (NDT), which are particularly suitable when dealing with structures and infrastructures because they allow one to not interfere with the state of the asset.
Most of NDT for structural element, like ultrasonic, magnetic field and eddy current methods, are mainly suited for the detection of defects at depths between 5 and 100 cm and they have two significant drawbacks: they need physical contact to the tested object and they generate images slowly by scanning. Infrared Thermography, also known as thermal inspection or infrared imaging, is a fast and remote method and it is becoming more widely used along with other NDT [1]. IRT is generally used for the non contact inspection of materials and it is characterized by the use of thermal and infrared sensors in order to visualize thermal surface contrast after a thermal excitation by flash or halogen lamps. Furthermore, IRT with a selective heating of the surface under investigation, permits to detect and to characterize the non-homogeneities in buildings structures in the near surface region up to a depth of about 10 cm [2].
Modeling thermal phenomena occurring during and after thermal excitation of structures is helpful to fully understand all the aspects of their thermal behavior, thus enhancing IRT effectiveness in internal structures detectability.
An experimental program has been started with the purpose of evaluating the reliability in building diagnosis and characterization of the integrated analysis of several parameters related to heat transfer process through the building material.
Experimental measurements using a thermal infrared detector have been carried out on a concrete structure with some defects. In this paper the finite element method has been applied to simulate the problem in order to detect the position of the defects.

2. Infrared Thermography

Infrared Thermography (IRT) is an effective tool for evaluating buildings condition, because it gives information with immediacy, rapidity and relatively low cost.
IRT is widely used for no-contact measurement of surface temperatures through infrared radiation emission. IRT measures the radiated electromagnetic energy in the infrared zone of the electromagnetic spectrum between 8 to 14 μm and produces 2D-images that represent heat wave contour.

Each object having a temperature higher than the absolute zero emits in the infrared spectrum and the emitted energy is proportional to the temperature. IRT application in the field of quality control of structural elements and materials is generally carried out by applying a thermal stimulation of the object under examination and then monitoring its surface temperature variation during the transient heating or cooling phase. The analysis involves heat conduction in solids [3].

The thermal energy propagates by diffusion under the surface while a thermal infrared camera monitors and records the temperature variation over the viewed surface. In case of homogenous material and uniform surface heating, temperature is uniformly distributed on the object under test.

The presence of a defect at a certain depth interferes with the heat flow causing local surface temperature variations or any other change in the thermal properties of the material [4]. The changes in heat flow cause localized energy differences on the surface of the test object, which can be measured using an infrared detector.

IRT is used for detecting subsurface characteristics such as subsurface thermal properties, presence of subsurface anomalies or defects. An infrared camera is generally used for creating fully analyzable images from the thermal radiation given off by the objects surface. A defect in the subsurface of the object can be revealed by a thermal anomaly in the distribution of temperature.

The emitted radiation can be focused through a special lens to a sensing element like a microbolometer focal plane array. The focal plane array generates a thermal image of the object called thermogram, starting from the electric signals. Thermograms are images in which colors represent surface temperatures according to a temperature scale.

IRT can be applied through active or passive approaches, depending on whether the inspected part is in thermal equilibrium or not. In passive Thermography instruments are used to analyze and record data without applying artificial heating or cooling to the object, thus allowing the evaluation of its temperature distribution due to both natural phenomena or heating developing during its ordinary life.

Active Thermography involves a deliberate change in temperature: a stimulus is directly applied to the object to cause heating or cooling [5]. In this work the second one technique will be analyzed.

3. Case study

The analysis of heating-up and cooling-down processes during and after activation with an external heat source is a well-established technique for the characterization of inhomogeneities in concrete and masonry structures [6, 7].

In this study a thermal analysis has been carried out on a small concrete wall with an inside cavity. The wall is 90 cm wide, 62 cm high and 38 cm thick. Using an empty box of polystyrene, a macro-cavity sized 20×38×14 cm^3 has been realized and assumed as a known anomaly. Moreover further defects realized with plastic discs with diameter of 7.5 cm and thickness of 0.3 cm have been inserted in the near surface of the structure at different depth, as shown in Figures 1 and 2.

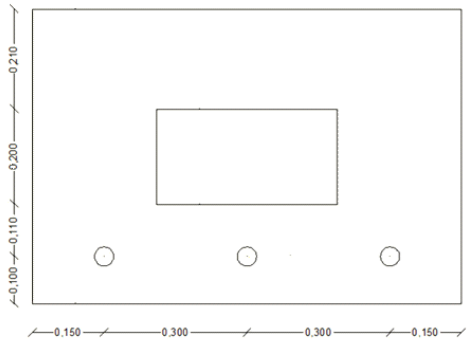

Figure 1. Front view of the wall (all the dimensions are in m).

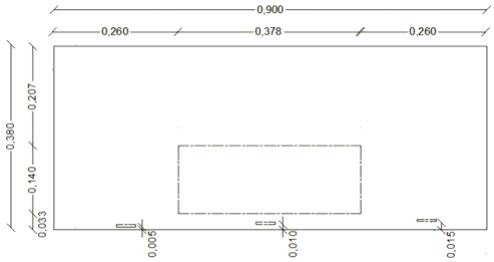

Figure 2. Horizontal section of the concrete wall (all the dimensions are in m).

The surface of the structure has been temporarily heated up with two halogen lamps with a power of 500 W by placing them at a distance of 1.5 m and at an angle of about 45° in respect to the concrete wall in order to homogenously heating the surface.
The heating-up duration was 9140 s whereas the cooling-down duration was 26820 s.
The temperature distribution during and after heating as a function of time has been recorded every 20 s using a thermal infrared detector Flir SC660 with a resolution of 640 × 480 pixels.

3.1 Experimental results

During the tests several thermograms have been acquired and recorded during both heating and cooling phase. The thermograms storage time (20 s) has been determined as a result of studies and attempts.
Selected thermograms of experimental data acquired at different time intervals during the heating up phase are shown in Figures 3-5. It can be noticed that the cavity and the other defects become more clear as the surface heating increases.
In the same way, Figures 6 and 7 show some thermograms concerning the cooling-down phase. The surface temperature decreases quickly and tends to show a quite uniform distribution.

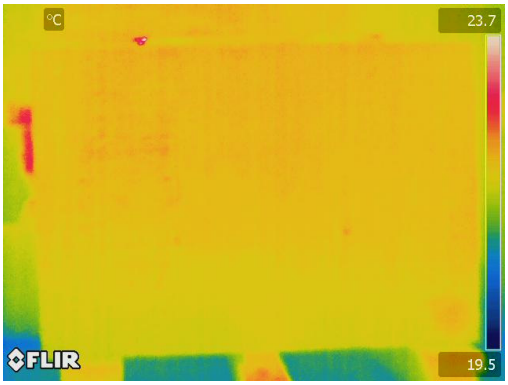

Figure 3. Thermogram acquired at the beginning of the heating-up phase.

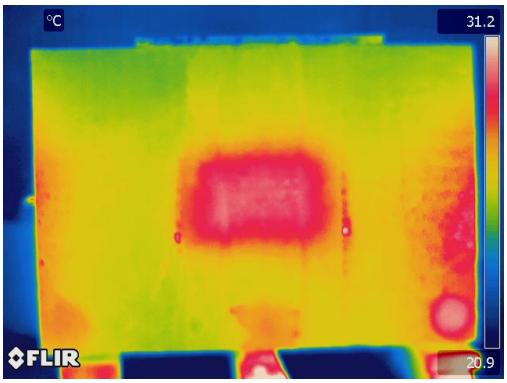

Figure 4. Thermogram acquired after 4570 s (heating-up phase).

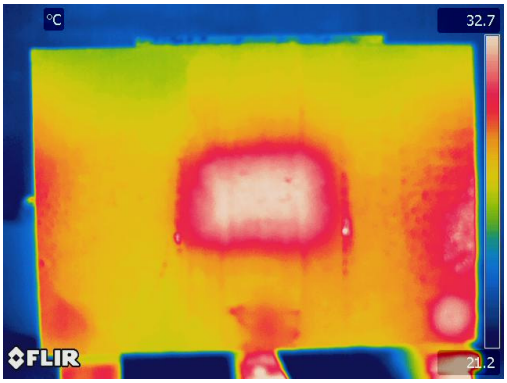

Figure 5. Thermogram acquired after 9140 s (heating-up phase).

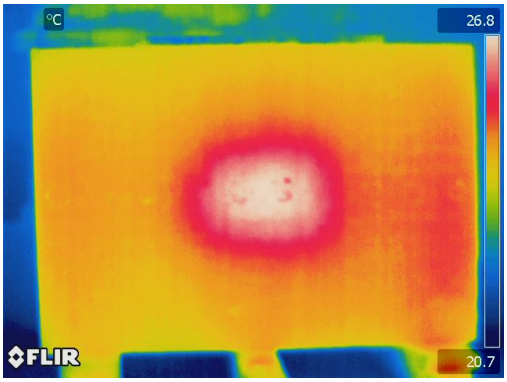

Figure 6. Thermogram acquired after 22550 s (cooling-down phase).

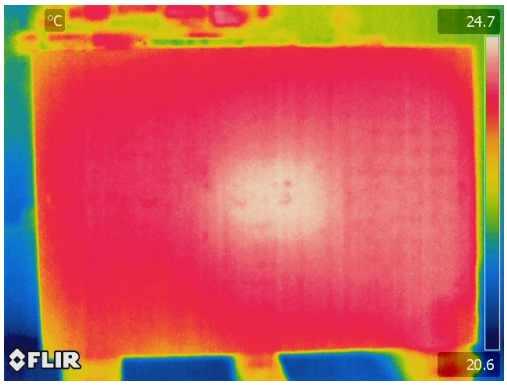

Figure 7. Thermogram acquired after 35960 s (cooling-down phase).

4. Numerical Model

A numerical model has been developed, with the Finite Element Method, using the Heat Transfer Module of COMSOL Multiphysics® in order to solve the problem of transient heat transfer occurring in experimental conditions. The influences of heat conduction, convection and radiation (surface to surface and surface to ambient) on the lateral heat flow through the defect, have been simulated and analyzed.

4.1 Governing Equations

The physical nature of the heat transfer is governed by the differential equations such as the one of the heat transfer by conduction, convection and radiation with temperature dependant thermal properties of materials involved.
The differential equation, governing pure conductive heat transfer, to be solved on the model domain is:

$$\rho C_p \frac{\partial T}{\partial t} - \nabla \cdot (k \nabla T) = 0 \quad (1)$$

where ρ is the density (kg/m^3), C_p is the material heat capacity at constant pressure (J/(kg·K)) T is absolute temperature (K) and k is the material thermal conductivity (W/(m·K)) and t is time.
The ambient temperature T_{amb} measured in the room was used both as boundary condition both as an initial condition since it was assumed that the wall was in equilibrium with the environment and therefore at room temperature before the experiment started. The initial condition is:

$$T(x, y, z, t = 0) = T_{amb} = 293.15[\mathrm{K}] \quad (2)$$

The boundary condition included heat transfer by convection and radiation from the object surfaces and the heat source q_0 applied on the front surface (during the first 9140 s in this case) is the following:

$$\mathbf{n}(k \nabla T) = q_0 + h_{conv}(T_{amb} - T) + \sigma\varepsilon(T_{amb}^4 - T^4) \quad (3)$$

where h_{conv} is the constant convective heat transfer coefficient, σ is the Stefan-Boltzmann constant and ε is the emissivity that is the ratio of radiant emittance of an object to that of a blackbody at the same temperature.
The emissivity ε is a numeric whose value lies from zero for a non radiating object and 1.0 for a blackbody.
Emissivity is a function of the type of material and its surface condition and can vary with wavelength and with the temperature of the object.
The Planck's law describes the spectral distribution of the radiation at a certain wavelength (spectral radiance) of a black body at different temperatures according to the following relationship:

$$W_{\lambda b} = \frac{2 \cdot \pi \cdot h \cdot c^3}{\lambda^5 \cdot \left(e^{h \cdot c / \lambda \cdot \sigma \cdot T} - 1\right)} \cdot 10^{-6} \left[W / m^2 \cdot \mu m\right] \quad (4)$$

where $W_{\lambda b}$ is the blackbody spectral radiant emmitance at the wavelength λ, c is the speed of light, h is the Planck's constant, and T is the absolute temperature of the blackbody.
The Wien's law can be determined by differentiation of Planck's law and permits to determine the maximum values of the spectral emittance versus the temperature:

$$\lambda_{\max} = \frac{2898}{T} \quad [\mu m] \quad (5)$$

where $\lambda_{\max}$ is the wavelength which corresponds to the maximum emittance.
In Eq. (3) second and third terms are accounting for the convection and radiation heat fluxes respectively.
In case of *surface to surface radiation* the following equation applies:

$$\mathbf{n}(k \nabla T) = \varepsilon(G - \sigma T^4) \quad (6)$$

where G is irradiation ($G = \sigma T_{amb}^4$ in the *surface to ambient radiation* case). Finally the following thermal insulation boundary condition implies that no convective heat transfer taking place:

$$\mathbf{n}(k\nabla T) = 0 \qquad (7).$$

4.2 Geometry, Model parameters and Mesh

The 3D model geometry (Fig. 8) is constituted by the concrete wall shown in Figures 1-2 and by two halogen lamps. The dimensions are the same of the experimental case study. Wall and halogen lamps are contained in a room with a constant temperature equal to 273.15 K. For this reason it is possible to omit the geometry of the room walls. Furthermore, the model assumes that this physical system is dominated by radiation and convection cooling. The model simulates the halogen lamps as two solid objects with a total heat source of 1000W. They are insulated on all surfaces except for the top, which faces the wall. At this surface, heat leaves the lamps as radiation only.
The model simulates the transient temperature field for 9140 s of heating and for 26820 s of cooling. The initial temperature is 273.15 K for all the objects.

The mesh consists of 12137 tetrahedral elements. An adjustment of the mesh parameters permits a different degree of mesh refinement in regions where larger temperature gradients were expected. The meshed model used can be seen in Figure 7.

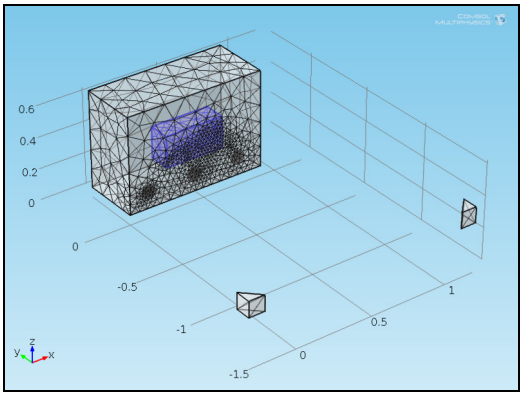

Figure 8. Meshed 3D model: concrete wall with inside air cavity (blue) and plastic discs and two halogen lamps.

Table 1 summarizes the material properties used in the model.

Table 1: Materials properties

	Plastic	**Concrete**	**Halogen Lamps**
Thermal Conductivity k **[W/(m·K)]**	0.23	1.8	400
Heat Capacity C_p **[J/(Kg·K)]**	1670	1000	10
Surface Emissivity ε		0.92	0.99
Density ρ **[Kg/m^3]**	1160	2300	8700

4.3 Numerical Results

A parametric analysis has been performed by varying the distance of the inside air cavity from the surface of the wall from 0.004 m to 0.05 m with step equal to 0.001 m. For each value of this distance a transient study from 0 s to 35960 s with a step size of 20 s has been computed with the aim of reproducing the same thermograms obtained experimentally.
The trend of the maximum value of the temperature versus the distance of the inside air cavity from the surface obtained after t=4570 s (blue) and t=9140 s (green) is shown in Figure 9. As can be noted, when the distance of the inside air cavity from the surface is equal to 0.009 m, the maximum value of the temperature is 32.7 °C for t = 9140 s and 31.3 °C for t = 4570 s.

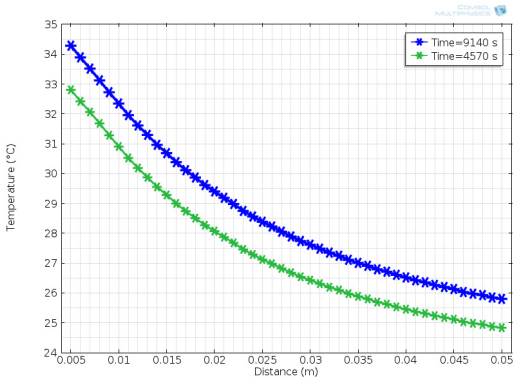

Figure 9. Trend of the maximum value of the temperature versus the distance of the inside air cavity from the surface.

These values are similar to those obtained experimentally in the thermograms shown in Figures 4 and 6, thus demonstrating that the inside air cavity is very close to the radiated surface of the concrete wall.
Figures 10-13 show the surface temperature distributions obtained when the distance of the inside air cavity from the surface is equal to 0.009 m. The temperature scale, varying from 20°C to 33°C, has been adjusted in order to match to that of the experimental data so that the images can be directly compared.
Simulated thermograms well match with experimental data.

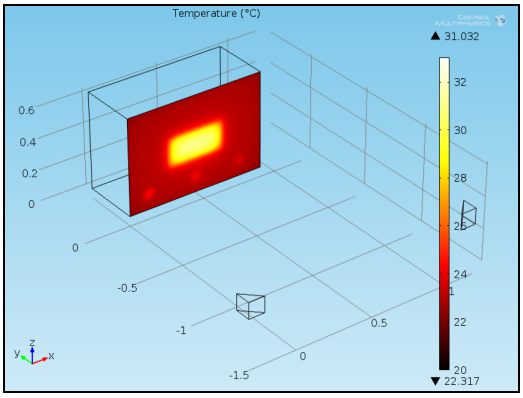

Figure 10. Simulated thermogram obtained after 4570 s with a distance of the inside air cavity from the surface of the wall equal to 0.009 m.

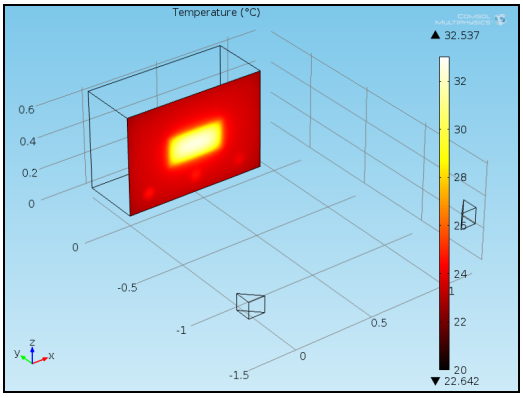

Figure 11. Simulated thermogram obtained after 9140 s with a distance of the inside air cavity from the surface of the wall equal to 0.009 m.

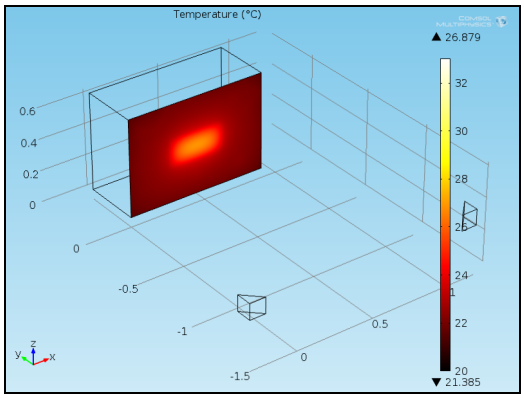

Figure 12. Simulated thermogram obtained after 22550 s with a distance of the inside air cavity from the surface of the wall equal to 0.009 m.

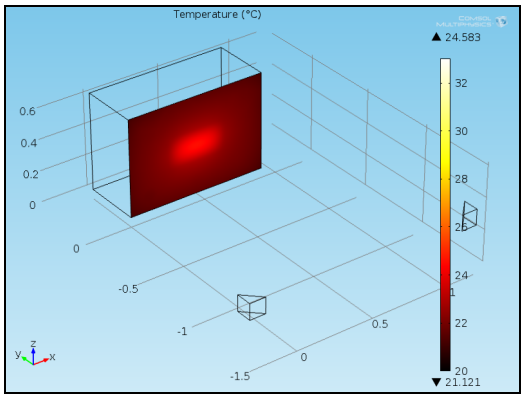

Figure 13. Simulated thermogram obtained after 36960 s with a distance of the inside air cavity from the surface of the wall equal to 0.009 m.

5. Conclusions

In this work a model of a concrete wall, already built and tested in the laboratory, has been implemented in order to simulate the heating propagation during infrared thermography tests.
Artificial defects, inserted in the near surface of the wall at different depth, have been detected in both experimental and simulated sessions.
Experimental data show that IRT is capable to evaluate with immediacy, rapidity and relatively low costs the condition of the tested wall.
Numerical data well match with the laboratory results and allow parametric studies freed from the experimental tests to be performed. The comparison of simulated and experimental thermograms allows the defect position to be identified.

Therefore, results show that the implemented COMSOL Multiphysics model is suitable to effectively simulate the thermal propagation process in the wall.

6. References

1. X. Maldague, *Theory and Practice of Infrared Technology for Non destructive Testing*. Wiley, New York (2001)
2. C. Maierhofer, R. Arndt, M. Röllig, C. Rieck, A. Walther, H. Scheel, B. Hillemeier, Application of impulse thermography for non-destructive assessment of concrete structures, *Cement & Concrete Composites*, **Vol. 28**, pp. 393-401 (2006)
3. H.S. Carslaw, J.C. Jaeger, *Conduction of Heat in Solids*. Clarendon Press, Oxford (1959)
4. C. Meola, A new approach for estimation of defects detection with infrared thermography, *Materials Letters*, **Vol. 61**, pp. 747-750 (2007)
5. P. O. Moore, X. Maldague, *NDT Handbook on Infrared technology ASNT Handbook Series*, ASNT Press (2001)
6. X. Maldague, *Non-destructive evaluation of materials by infrared thermography*. Spinger-Verlag, London (1993)
7. S. Danesi, A. Salerno, D. Wu, G. Busse, Cooling down thermography: principles and results in NDE, *Proceeding of the International society for optical engineering, Thermosense XX*, pp. 266-274 (1998)

7. Acknowledgements

This work is supported by the operating program of Regione Sardegna (European Social Fund 2007–2013), L.R.7/2007, "Promotion of scientific research and technological innovation in Sardinia".